The interaction between C35 and ΔNp73 promotes chemo-resistance in ovarian cancer cells

TH-Y Leung[1], SC-S Wong[1], KK-L Chan[1], D W Chan[1], AN-Y Cheung[2] and HY-S Ngan*,[1]

[1]Department of Obstetrics and Gynaecology, LKS Faculty of Medicine, The University of Hong Kong, Pokfulam, Hong Kong Special Administrative Region and [2]Department of Pathology, LKS Faculty of Medicine, The University of Hong Kong, Pokfulam, Hong Kong Special Administrative Region

Background: The purpose of this study was to characterise the oncogenic roles of C35, a novel protein binding partner of ΔNp73, in ovarian cancer and to investigate the functional significance of C35–ΔNp73 interaction in the regulation of chemo-resistance.

Methods: C35 expression was evaluated by quantitative real-time PCR in human ovarian cancer tissues and cell lines. The aggressiveness of ovarian cancer cells overexpressing C35 was examined by cell proliferation, migration, soft agar and nude mouse xenograft. The significance of C35–ΔNp73 interaction in chemo-resistance was evaluated by apoptosis assays and cell viability after cisplatin treatment.

Results: The expression of C35 was significantly enhanced in human ovarian cancer tissues. Overexpression of C35 augmented proliferation, migration and tumourigenicity in ovarian cancer cell lines. C35 knockdown inhibited cell motility and cell growth. The co-expression of C35 and ΔNp73 by transient or stable transfection in ovarian cancer cells induced greater resistance to cisplatin treatment than did transfection with C35 or ΔNp73 alone. The cisplatin resistance was demonstrated to be caused by increased AKT and NFκB activity induced by C35–ΔNp73.

Conclusion: Our results suggest that ΔNp73 might cooperate with C35 to promote tumour progression and contribute to cisplatin resistance in ovarian cancer cells. Future studies of the functional roles of ΔNp73 and C35 will provide insight that will aid in the establishment of new strategies and more effective therapies.

Ovarian cancer is one of the most common causes of cancer death in women in western countries and Southeast Asia, including Hong Kong. However, the molecular mechanisms underlying the progression of ovarian cancer remain obscure. p73 has been suggested to have a role in an alternative p53-independent apoptotic pathway in ovarian cancer. p73 is expressed in two major forms: an N-terminal transactivation domain-containing isoform (TAp73) and a dominant-negative isoform that lacks the transactivation domain (ΔNp73) (Kaghad et al, 1997). TAp73 exhibits growth-inhibitory, tumour-suppressive and pro-apoptotic functions, whereas ΔNp73 forms complexes with TAp73 and p53, effectively abolishing the tumour suppressor functions of TAp73

and p53 (Zaika et al, 2002). Several studies have suggested that the expression of TAp73 enhances cisplatin-induced apoptosis by upregulating genes such as *p21* and *Bax* in ovarian cancer cells (Muscolini et al, 2008; Righetti et al, 2008; Al-Bahlani et al, 2011). Evidence from our previous observations has demonstrated that the radiosensitivity of cervical cancer is associated with the expression of TAp73 and ΔNp73, and these results indicate that p73 might have an important role in controlling cellular radiosensitivity (Liu et al, 2006). We also showed that the interaction of TAp73 with breast cancer-associated gene 3 (BCA3) enhanced the radiosensitivity of cervical cancer cells and documented the importance of TAp73 in the treatment of cervical

cancer (Leung and Ngan, 2010). Therefore, it is speculated that the interaction of p73 with other signalling proteins might contribute to its function in response to cancer treatment. To further investigate the molecular mechanisms of p73, we searched for potential interaction partners by performing a yeast two-hybrid screen using a HeLa cDNA library. We identified C35, also known as MIEN1, as a potential protein partner of p73. C35 is a novel protein that has an important role in cancer progression and metastasis (Katz et al, 2010; Dasgupta et al, 2011). Although C35 has functional roles in different cancers, the detailed mechanisms underlying its functions remain largely unclear. The identification of C35 as a novel interacting partner of p73 prompted us to investigate the significance of this interaction.

Our data showed that C35 has a significant oncogenic role in ovarian cancer, promoting cell growth, cell migration and transformation. We also confirmed that C35 preferentially interacts with ΔNp73 using co-immunoprecipitation and immunofluorescence staining. When C35 was co-expressed with ΔNp73, the level of apoptosis of ovarian cancer cells in response to cisplatin treatment was largely reduced. The reduction of this response was due to the activation of AKT and an increase in NFκB activity. Our data strongly suggest that ΔNp73 acts synergistically with C35 via their binding to induce tumour formation and to mediate chemotherapy resistance. This study is the first to demonstrate the collaborative roles of C35 and ΔNp73 in the tumour progression and chemo-resistance of ovarian cancer.

MATERIALS AND METHODS

Yeast two-hybrid screening. Yeast two-hybrid screening was performed as described previously (Leung and Ngan, 2010). Positive colonies were isolated, and the plasmid DNA in the yeast was prepared and transformed into Escherichia coli DH5α. Direct sequencing was performed to determine the identities of the potential protein interacting partners of ΔNp73.

Plasmid construction. The full-length coding region of C35 was amplified by PCR with gene-specific primers containing an EcoRI restriction site. The PCR products were digested with EcoRI and subsequently cloned into the pcDNA3.1 + expression vector, which encodes a Myc epitope. The full-length coding region of TAp73 and ΔNp73 was amplified by PCR with gene-specific primers containing HindIII restriction site. The PCR products were digested and cloned into the pEGFP expression vector. ΔNp73 1–198, ΔNp73 1–400 and ΔNp73Δ1–76 were prepared by PCR amplification with primers at the indicated position of ΔNp73 and cloned into the pEGFP expression vector.

Site-directed mutagenesis of C35. Site-directed mutagenesis was performed to generate C35 Y39F/Y50F. Specific mutations were generated by two rounds of three-step PCR. The first-round PCR was performed using primer set: F: 5′-GAGGCGACCTTCCTG GAGCTG-3′ and R: 5′-CAGCTCCAGGAAGGTCGCCTC-3′ to generate C35 Y39F using pcDNA3.1 + C35 as a template. The second-round PCR was then performed on C35 Y39F with primer set: F: 5′-AAGGAGCAGTTTCCGGGCATC-3′ and R: 5′-GATGCCCGGAAACTGCTCCTT-3′ to generate C35 Y39F/Y50F. The final PCR product was cloned into pcDNA3.1 + vector.

Cell lines. Three immortalised human ovarian surface epithelial (HOSE) cell lines, HOSE11-24-96, HOSE17-1 and HOSE96-9-18 (Tsao et al, 2001) (gifts from Prof. GSW Tsao, Department of Anatomy, The University of Hong Kong); the ovarian epithelial cancer cell lines OV2008, C13, A2780S and A2780CP (Sasaki et al, 2000; Asselin et al, 2001) (gifts from Prof. BK Tsang, Department of Obstetrics and Gynaecology, University of Ottawa); the ovarian cancer cell lines OV326, OV429, OV420, OV433 and SKOV-3; and

HEK293 human embryonic kidney cells (purchased from the American Type Cell Collection, Rockville, MD, USA) were used in this study. All cells were maintained in DMEM or MEM supplemented with 10% FBS and 100 units of penicillin/streptomycin.

Co-immunoprecipitation. Myc-tagged C35 was co-transfected with GFP-tagged ΔNp73, GFP-tagged TAp73 or GFP-tagged p53 into HEK293 cells using Lipofectamine 2000 (Invitrogen, Carlsbad, CA, USA). Transfected cells were lysed with NET lysis buffer containing 0.2% NP-40. The cell lysates were then incubated with an anti-Myc antibody, and the immunoprecipitates were collected using protein G Sepharose (GE Healthcare, Buckinghamshire, UK). The total cell lysates and the immunoprecipitates were subjected to SDS gel electrophoresis and western blotting. Anti-Myc and anti-GFP antibodies (Santa Cruz, Dallas, TX, USA) were used to detect Myc-tagged C35 and GFP-tagged ΔNp73/TAp73/p53, respectively.

Western blot analysis. Proteins were analysed by western blot using antibodies including p53 (Santa Cruz), ΔNp73 (Novus, Littleton, CO, USA), AKT (Cell Signaling, Danvers, MA, USA), p-AKT (Cell Signaling) and NFκB p65 (Cell Signaling) and a horseradish peroxidase-conjugated secondary antibody. Antibody binding was detected with enhanced chemiluminescence (ECL). β-Actin or GAPDH (Sigma, St Louis, MO, USA) was probed as a loading control of total cell lysate while c-Jun (Cell Signaling) and α/β tubulin (Cell Signaling) were probed as a loading control of nuclear fraction and cytosolic fraction, respectively.

Protein stability assay. To determine the stability of C35, Myc-tagged C35 together with GFP vector or GFP-tagged ΔNp73 was transiently transfected into 293 cells. Twenty-four hours after transfection, cells were treated with cycloheximide ($100 \mu g \, ml^{-1}$). Cell lysates from different time points (0–12 h) were collected and analysed by western blotting.

Immunofluorescence staining. Cells were seeded onto coverslips and transfected with the Myc-tagged C35 plasmid alone or together with a GFP-tagged p73 plasmid. Immunofluorescence staining was performed as described previously (Leung et al, 2005). Nuclei were stained with DAPI.

Establishment of stable C35-expressing clones. OV2008 cells were transfected with Lipofectamine 2000 (Invitrogen) and $3 \mu g$ of the DNA construct according to the manufacturer's instructions. The transfected OV2008 cells were selected and maintained in complete medium containing G418 at $1 \, mg \, ml^{-1}$ (Calbiochem, Schwalbach, Germany). Cells stably expressing C35 or control vector were then isolated, and the expression of C35 was confirmed by western blotting using an anti-Myc antibody (Santa Cruz). Three C35 stable clones were established and named as OV-C35-M1, OV-C35-M2 and OV-C35-M3. Two empty vector (pcDNA3.1 +) stably transfected clones were generated as a control (OV-MV1 and OV-MV2).

Cell proliferation assay. An XTT assay was performed using the Cell Proliferation Kit II (Roche Applied Science, Indianapolis, IN, USA) according to the manufacturer's protocol. Approximately 1200 cells were seeded onto a 96-well plate. Cell growth was evaluated daily for 3 days. The culture medium was removed, and the cells were washed with $100 \mu l$ of $1 \times$ PBS (Gibco, Paisley, UK). The cells were subsequently resuspended in $100 \mu l$ of $1 \times$ PBS, and $50 \mu l$ of XTT labelling reagent and $1 \mu l$ of electron coupling reagent were added to the suspended cells. The cells were incubated in a $37 \, ^{\circ}C$ humidified incubator for 4 h, after which time the absorbance (A_{492}) was measured.

Cell migration assay. For the cell migration assay, 1×10^5 cells were resuspended in $100 \mu l$ of serum-free medium and seeded into the top chambers of 8-μm-pore, 6.5-mm polycarbonate transwell

inserts (Corning, NY, USA); 600 μl of complete medium was added to the bottom chamber. The cells were then allowed to migrate for 8–16 h. The cells were fixed and stained, and the number of migrated cells on the lower surface of the inserts was quantified with Image-Pro Plus software (Media Cybernetics, Rockville, MD, USA).

Soft agar assay. For the soft agar assay, 2×10^4 cells were suspended in 2 ml of medium (MEM supplemented with 10% FBS) containing 0.4% agar. The cell mixture was then seeded on a layer of 1% bottom agar in a 60-mm plate and allowed to grow for 4 weeks. The assay was performed in triplicate for each cell line. After 4 weeks of incubation, colonies were counted in five fields for each plate.

Nude mouse xenograft assay. Approximately 1×10^6 cells in 0.1 ml of PBS were injected subcutaneously into the flanks of BALB/C nude mice. The sizes of the subcutaneous tumours formed in the nude mice were measured and recorded every 3 days. After 6 weeks, the mice were killed, and the tumours were excised and weighed. The animal work was performed according to the Animals (Control of Experiments) Ordinance (Hong Kong) and followed the relevant university guidelines. The research protocol (CULATR 1987-09) was approved by the University Committee on the Use of Live Animals in Teaching and Research (CULATR).

Small interfering RNA. The small interfering RNA (siRNA) targeting C35 and the non-targeting control (NTC) siRNA were purchased from Applied Biosystems Inc. (Foster City, CA, USA). The transfections with the C35 siRNA and the NTC siRNA (50 pmol in 2 ml of medium) in six-well plates were performed using Lipofectamine 2000 (Invitrogen) according to the manufacturer's instructions.

Cell viability assay. Cell viability was evaluated by Trypan blue dye exclusion assay 24 h after treatment with DMSO or different concentrations of cisplatin (0, 10, 20 and 50 μM). Briefly, cells were washed, trypsinzed and mixed with Trypan blue dye for 5 min. The number of Trypan blue-stained cells (dead cells) and transparent cells (live cells) were counted by Luna automated cell counter (Logos Biosystems, Annandale, VA, USA). The assay was performed in triplicate.

Nuclear NFκB p65 ELISA. Nuclear protein was extracted using the Nuclear Extraction Kit (Panomics Inc., Santa Clara, CA, USA). The NFκB p65 ELISA kit (Panomics Inc.) was used according to the manufacturer's instructions. Briefly, 5 μg of nuclear extracts from each sample was transferred to the 96-well plate containing the consensus NFκB sequence. Samples were incubated at room temperature for 1 h on rocking shaker. The NFκB p65, bound to the oligonucleotide, was detected by incubation with NFκB p65 antibody and then followed by horseradish peroxidase-conjugated secondary antibody. Tetramethylbenzidine (TMB) substrate was added to provide a colorimetric readout and the reaction was stopped by stop solution. The signal in each sample was quantified by measuring the absorbance of 450 nm by spectrophotometer. The assay was performed in triplicate.

Subcellular fractionation. Transfected cells were washed and collected by trypsinisation. The cell pellet was resuspended in cold HEPES buffer containing 10 μM HEPES, 10 mM KCl, 0.1 mM EDTA, 0.1 mM EGTA and 1 mM DTT supplemented with 0.5 mM PMSF and protease inhibitors. Ten percent of NP-40 was added to cell suspension and vortexed vigorously for 10 s, followed by centrifugation in a microfuge for 30 s. The supernatant containing the cytosolic fraction was collected. The nuclear pellet was resuspended in cold HEPES buffer containing 20 mM HEPES, 0.4 M NaCl, 1 mM EDTA, 1 mM EGTA, and 1 mM DTT supplemented with 1 mM PMSF and protease inhibitors. The resuspended pellet was then kept on ice for 15 min followed by

centrifugation for 5 min. The supernatant containing the nuclear fraction was collected. Protein concentrations of the cytosolic and nuclear fractions were determined by Bradford assay (Bio-Rad, Hercules, CA, USA), and equal amounts of cytosolic and nuclear proteins were subjected to western blot analysis.

Collection of ovarian cancer clinical samples and control specimens. Samples from 94 ovarian cancer tissues and 46 normal ovarian tissues were collected at the Department of Obstetrics and Gynaecology, Queen Mary Hospital, The University of Hong Kong. These samples were surgically resected and immediately snap frozen in liquid nitrogen. Written informed consent was obtained from patients, and the collection and use of tumour samples was approved by the local institutional ethics committee (Institutional Review Board number: UW 05-143 T/806).

Quantitative real-time PCR. Total RNA samples were isolated using the TRIzol reagent according to the manufacturer's protocol (Invitrogen). cDNA was synthesised from 1 μg of total RNA using High Capacity RNA-to-cDNA Master Mix (Applied Biosystems Inc.). Quantitative real-time PCR was performed using the Applied Biosystems TaqMan system. TATA-box binding protein (TBP) was used as an internal control.

Apoptosis assay. OV2008 cells in a 96-well plate were transfected with different combinations of plasmids. Twenty-four hours after transfection, the cells were treated with cisplatin (10 μM) and allowed to grow for 72 h. An apoptosis assay (*In Situ* Cell Death Detection Kit, Roche, Mannheim, Germany) was performed to study the apoptotic response of the cells to cisplatin. The percentage of apoptotic cells was determined as the percentage of GFP-positive cells that were also positively stained with TMR red. At least 200 GFP-positive cells were counted for each experiment.

RESULTS

The identification of C35 as a protein binding partner of ΔNp73. To obtain greater insight into the role of p73 in the development of ovarian cancer, we used a yeast two-hybrid assay to screen a HeLa cDNA library using full-length ΔNp73 as the bait. DNA sequencing analysis showed that one of the positive clones was a full-length clone of C17ORF37, that is, C35 (GI: 42822890). The physical interaction between C35 and ΔNp73 was confirmed by co-immunoprecipitation. In addition, the binding of C35 with the transactivation domain-containing form of p73 (TAp73) and p53 was also tested. C35 was able to interact with ΔNp73 but not with TAp73, p53 or the vector control in HEK293 cells (Figure 1B). The C35 binding site in ΔNp73 was then mapped using ΔNp73 C-terminal truncation constructs (ΔNp73 1–198 and ΔNp73 1–400) and a ΔNp73 N-terminal truncation construct (ΔNp73Δ1–76). We found that C35 was able to bind to ΔNp73 1–198 and ΔNp73 1–400 but not to ΔNp73Δ1–76 (Figure 1C). Because the immunoreceptor tyrosine-based activation motif (ITAM) is important for cell transformation (Katz *et al*, 2010), we also included the C35 Y39F/Y50F mutant in the co-immunoprecipitation assay. We found that ΔNp73 physically interacted with the C35 Y39F/Y50F mutant, indicating that the ITAM of the C35 protein does not contribute to the interaction between the two proteins (Figure 1C). Because the only difference between ΔNp73 and TAp73 is the presence of the first 13 amino acids at the N-terminus of ΔNp73 (Figure 1A), these results suggest that C35 preferentially binds to ΔNp73 through the N-terminal region.

The co-localisation and interaction of ΔNp73 and C35 *in vivo*. Previous studies have reported that C35 is primarily localised to the cytoplasm in prostate cancer cells (Dasgupta *et al*, 2009). Our immunofluorescence staining also demonstrated that ectopically expressed C35 localised to the cytoplasm (Figure 1D
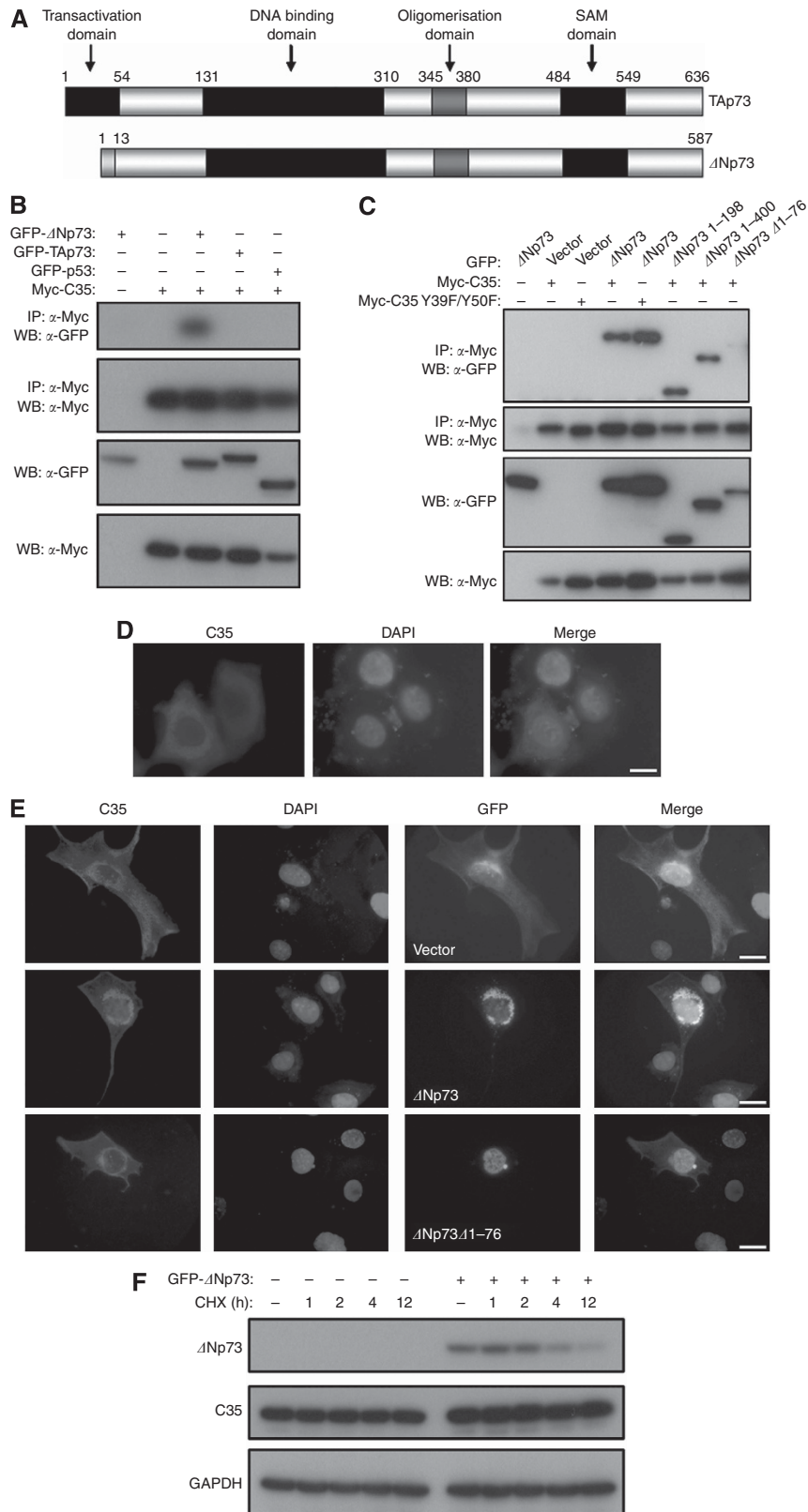
Figure 1. (**A**) The domain structures of TAp73 and ΔNp73. (**B**) The interaction between GFP-ΔNp73 and Myc-C35 in HEK293 cells was demonstrated by co-immunoprecipitation. (**C**) The interactions of Myc-C35 and Myc-C35 Y39F/Y50F with GFP-ΔNp73 and different GFP-ΔNp73 truncation constructs were examined by co-immunoprecipitation. (**D**) and (**E**, upper panel) The localisation of Myc-tagged C35 in the ovarian cancer cell line OV2008 was evaluated using an anti-Myc antibody. (**E**) The co-localisation of C35–ΔNp73 with the peri-nuclear region in OV2008 cells is indicated by yellow colour in the immunofluorescence images (middle panel). The co-staining of C35 and a ΔNp73 N-terminal truncation mutant (ΔNp73Δ1–76) is shown in the lower panel. Scale bar = 10 μm. (**F**) Myc-C35 was co-transfected with GFP vector or GFP-ΔNp73. After transfection, cells were treated with 100 μg ml^{-1} cycloheximide and harvested at time points ranging from 0 to 12 h. The expression of ΔNp73 and C35 was detected by anti-GFP and anti-Myc antibodies. GAPDH was probed as a loading control. A full colour version of this figure is available at the *British Journal of Cancer* journal online.

and E, upper panel). OV2008 cells transiently co-expressing C35 and ΔNp73 also exhibited co-localisation of C35 and ΔNp73 at the peri-nuclear region (Figure 1E, middle panel). No co-localisation was observed in C35 and ΔNp73Δ1–76 co-expressing cells (Figure 1E, lower panel). Furthermore, to determine the stability of C35 protein in ovarian cancer cells, Myc-tagged C35 together with GFP vector or GFP-tagged ΔNp73 was transiently transfected into 293 cells. The degradation rate of C35 was examined after exposure to cycloheximide ($100\,\mu g\,ml^{-1}$) (protein biosynthesis inhibitor) with different time durations. We found that C35 is a stable protein that could express 12 h after cycloheximide treatment (Figure 1F, left panel). We also observed that ΔNp73 is relatively unstable and could be degraded after exposure to cycloheximide. No obvious change in C35 protein stability was observed in ΔNp73- and C35-co-transfected 293 cells (Figure 1F, right panel).

C35 expression in normal ovarian and ovarian cancer cell lines and human tissue samples. Quantitative real-time PCR was performed to evaluate the mRNA expression of C35 in a panel of normal ovarian and ovarian cancer cell lines. In general, higher C35 expression was detected in the ovarian cancer cell lines than in the normal ovarian cell lines (HOSE11-24-96, HOSE17-1 and HOSE96-9-18) (Figure 2A). In addition, we also assessed the mRNA expression of C35 in 42 normal ovarian tissue samples and 94 ovarian tumour tissue samples and found that C35 was significantly overexpressed in the tumour samples relative to the expression levels in the normal tissues ($P < 0.0001$, Mann–Whitney Test, Figure 2B). Since the expressions of p53 and ΔNp73 have been suggested to have a role in chemosensitivity, we performed western blot to examine the endogenous expression levels of p53 and ΔNp73 in two ovarian cancer cell lines A2780S and OV2008 and their derivative cisplatin-resistant sublines A2780CP and C13 before and after cisplatin ($10\,\mu M$) treatment. Low levels of ΔNp73 were detected in A2780S and A2780CP whereas higher ΔNp73 expressions were found in OV2008 and C13. Expressions of p53 were detected in all cell lines. However, no obvious change in

protein expression of p53 and ΔNp73 was observed in the absence and presence of cisplatin treatment (Figure 2C) and no correlation between the expression of ΔNp73 and C35 was found in these two pairs of cell lines.

C35 enhanced cell proliferation and the *in vitro* and *in vivo* tumourigenicity of ovarian cancer cells. To study the *in vivo* function of C35 in ovarian cancer, we established OV2008 ovarian cancer cells that overexpress Myc-tagged C35. Three stable C35-overexpressing clones were established and verified by western blot using an anti-Myc antibody (Figure 3A). The stable expression of C35 enhanced the cell proliferation rates of all the three C35-overexpressing clones as determined by the XTT assay (Figure 3B). To determine whether the tumourigenicity of OV2008 ovarian cancer cells could be enhanced by C35, an anchorage-independent soft agar assay was performed. All stable C35-transfected clones formed larger colonies in soft agar than did control clones within the same period of time (Figure 3D). The numbers of colonies formed by OV-C35-M1 cells ($P = 0.0002$, *t*-test), OV-C35-M2 cells ($P = 0.0015$, *t*-test) and OV-C35-M3 cells ($P = 0.001$, *t*-test) were significantly higher than the numbers of colonies formed by the controls (Figure 3C). To further investigate whether C35 also augments the tumourigenicity of ovarian cancer cells *in vivo*, OV-C35-M3, OV-MV1 and parental OV2008 cells were subcutaneously injected into immunodeficient mice. The sizes of the xenografts were monitored and recorded for 6 weeks (Figure 3E). The tumours formed by OV-C35-M3 cells were significantly larger ($P > 0.01$) and heavier ($P > 0.05$) than those formed by OV-MV1 and parental OV2008 cells (Figure 3F and G). These data indicated that C35 enhances tumourigenicity by positively regulating cell growth.

C35 regulated cell migration and chemo-resistance in ovarian cancer cells. It has been reported that C35 contributes to prostate cancer cell migration and invasion (Dasgupta *et al*, 2009). To explore the effects of C35 on cell motility in ovarian cancer, a transwell migration assay was performed with stable
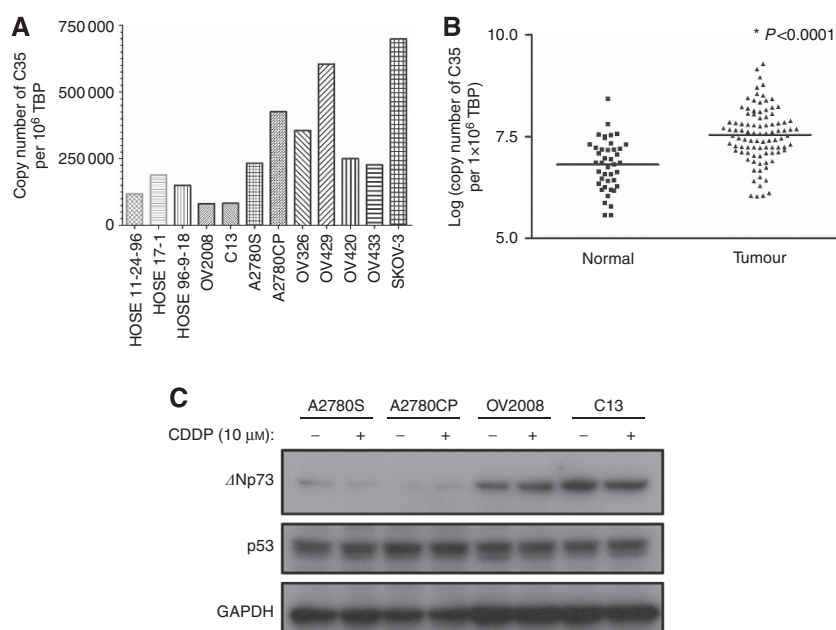

Figure 2. (**A**) The expression of C35 mRNA in ovarian cancer cell lines and human ovarian surface epithelial (HOSE) cell lines was evaluated by quantitative real-time PCR. The housekeeping gene TBP was used as an internal control. (**B**) The expression of C35 mRNA in normal ovarian tissues ($n = 46$) and ovarian cancer tissues ($n = 94$). C35 was significantly overexpressed in the clinical tumour samples ($P < 0.0001$). (**C**) Endogenous expressions of p53 and ΔNp73 in A2780S, A2780CP, OV2008 and C13 in the absence and presence of cisplatin were examined by western blot. GAPDH was probed as a loading control.
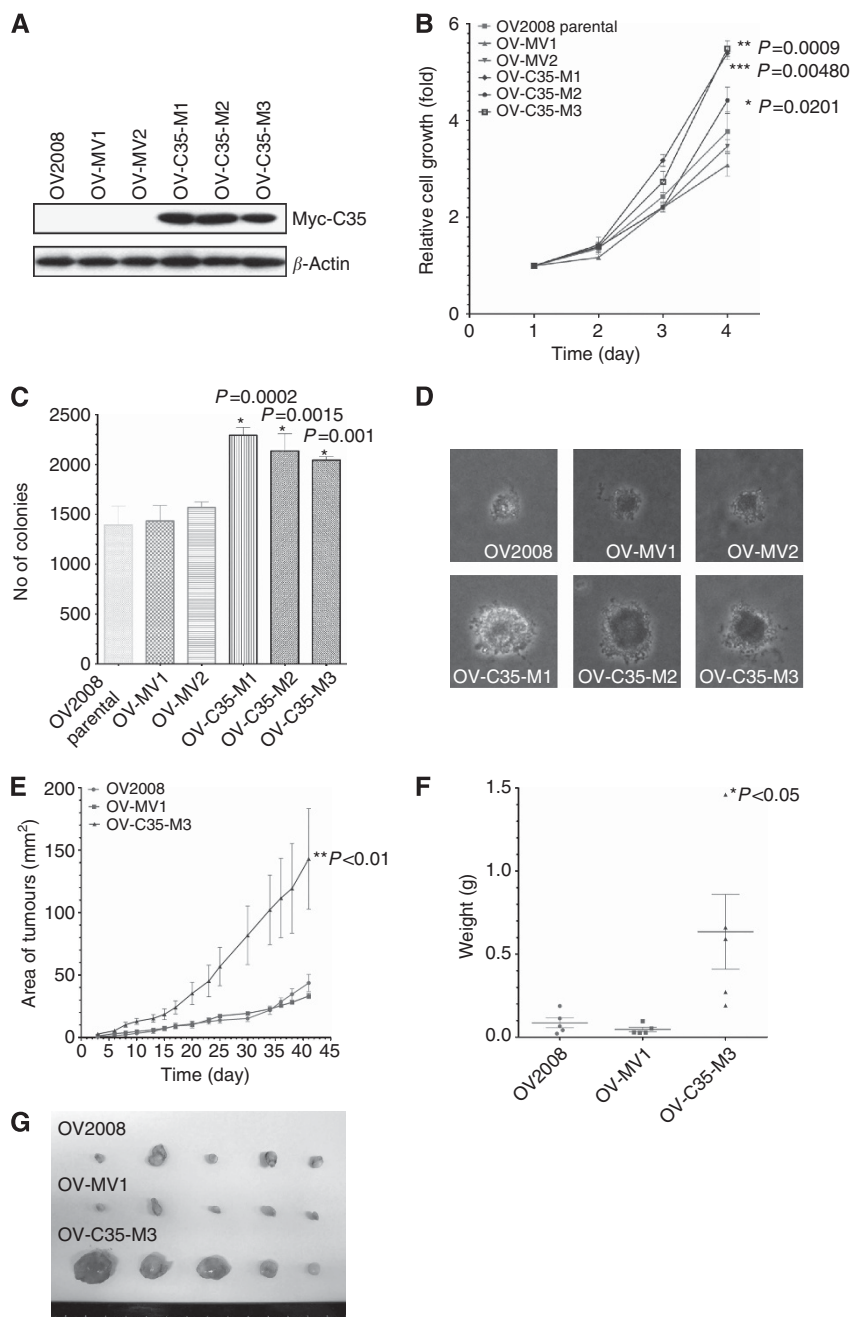
Figure 3. (**A**) OV2008 cells stably expressing Myc-tagged C35 were established. The expression of C35 in OV-C35-M1, OV-C35-M2 and OV-C35-M3 cells was confirmed by western blotting using an anti-Myc antibody. (**B**) The proliferation rates of stable C35-overexpressing clones of OV2008. The relative cell growth (normalised to day 1) was examined by XTT assays over 4 days. The proliferation rate was significantly enhanced in the stable C35-overexpressing clones (OV-C35-M1, $P=0.0009$; OV-C35-M2, $P=0.0201$ and OV-C35-M3, $P=0.0048$) compared with the control vector clones and parental OV2008 cells. (**C** and **D**) C35 enhanced the *in vitro* tumourigenicity of OV2008 cells, as demonstrated by soft agar assays. Stable C35-overexpressing clones formed more and larger colonies than the control vector clones and the parental OV2008 cells. (**E**) C35 enhanced tumourigenicity *in vivo*, as confirmed by nude mouse xenograft assays. After inoculation, the size of the tumours was measured every 2–3 days. Tumours formed by stable C35-overexpressing clones were significantly larger than those formed by control stable clones, OV-MV1 cells and parental OV2008 cells ($P<0.01$). (**F**) The excised tumours formed by OV-C35-M3 cells were significantly heavier than those formed by OV-MV-1 and parental OV2008 cells ($P<0.05$). (**G**) The excised tumours formed by OV-C35-M3 cells were larger than those formed by OV-MV1 and parental OV2008 cells.

C35-overexpressing clones. Cell migration was significantly enhanced in all three C35-overexpressing clones compared with OV-MV1, OV-MV2 and parental OV2008 cells (Figure 4A, $P<0.001$, $P<0.01$ and $P<0.05$, *t*-test). To further determine the physiological importance of C35 in regulating cell motility, we used siRNA to knockdown endogenous C35 expression in SKOV-3 cells (which have high C35 expression). The C35 siRNA profoundly reduced the level of C35 mRNA expression, by ∼70%, in SKOV-3 cells relative to the expression level in cells transfected with non-target control (NTC) siRNA (Figure 4B). We also evaluated the knockdown efficiency in SKOV-3 cells that were co-transfected with (1) NTC siRNA + pcDNA3.1 + Myc C35 or (2) C35 siRNA +
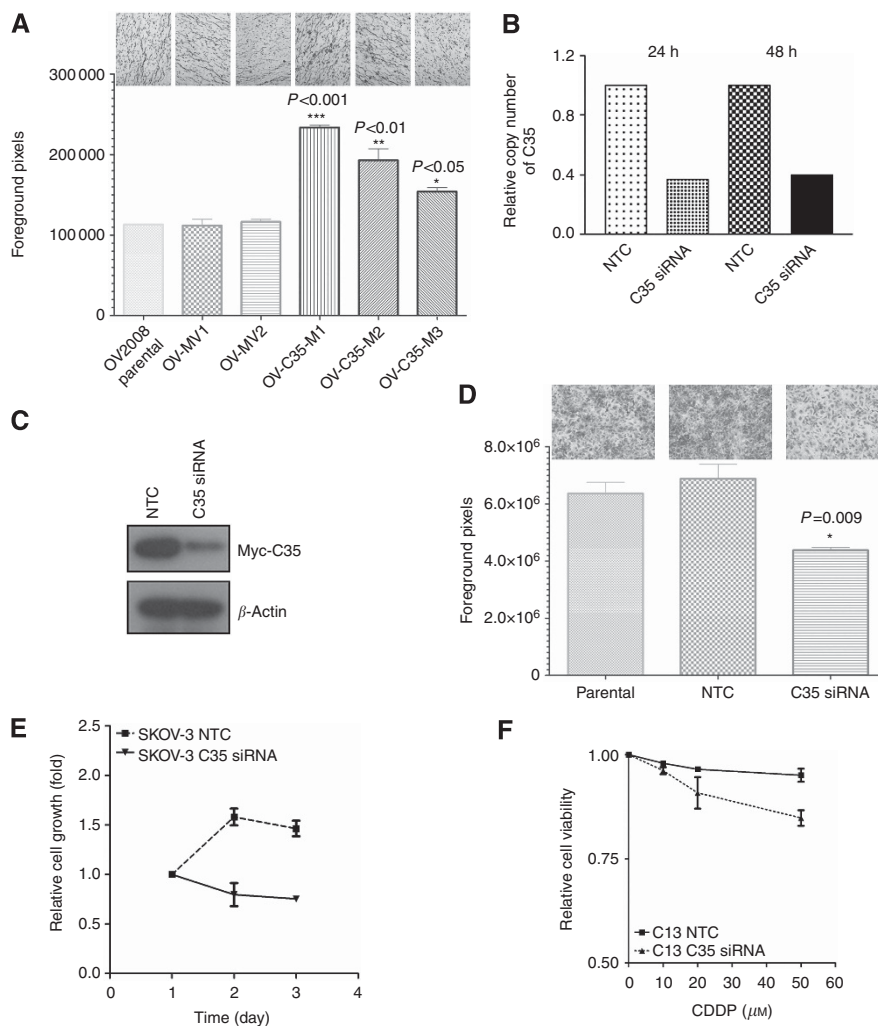
Figure 4. (A) Transwell migration assay of stable C35-overexpressing clones. A transwell migration chamber was used to examine the migration capacity of OV-C35-M1, OV-C35-M2, OV-C35-M3, OV-MV1, OV-MV2 and parental OV2008 cells. Migrated cells were stained and counted. The migration assay showed that the overexpression of C35 promoted cell migration in OV2008 ovarian cancer cells. (B) Real-time PCR was performed to measure C35 mRNA expression in C35 siRNA- and NTC siRNA-transfected SKOV-3 cells at 24 and 48 h after transfection. (C) Western blotting with an anti-Myc antibody was performed to evaluate the expression of Myc-C35 in NTC siRNA- and C35 siRNA-transfected SKOV-3 cells. β-Actin was probed as a loading control. (D) The downregulation of C35 inhibited the cell migration. SKOV-3 cells were transfected with NTC siRNA or C35 siRNA. Transfected cells were then subjected to transwell migration assays. The number of migrated C35 siRNA-transfected cells was significantly reduced compared with the number of migrated NTC siRNA-transfected cells ($P = 0.009$). (E) SKOV-3 cells were transfected with NTC siRNA or C35 siRNA. The effect on cell proliferation over a period of 3 days after cisplatin ($10\,\mu M$) treatment was evaluated by XTT assays. (F) Chemo-resistant ovarian cancer cell line C13 cells were transfected with NTC siRNA or C35 siRNA. Transfected cells were treated with different concentrations of cisplatin (0, 10, 20 and $50\,\mu M$). Cell viability was examined by Trypan blue exclusion assay.

pcDNA3.1 + Myc C35. Western blot analysis revealed that the C35 siRNA dramatically suppressed the expression of Myc-C35. These results confirmed that the C35 siRNA effectively silenced the expression of the C35 protein (Figure 4C). After siRNA transfection, a transwell migration assay was performed. The C35 siRNA significantly reduced the number of migrated cells, whereas the NTC siRNA had no effect (Figure 4D) ($P = 0.009$, t-test). Moreover, the effect of the siRNA knockdown of C35 on the response of ovarian cancer cells to cisplatin treatment was also evaluated. As shown in Figure 4E, XTT assays revealed that the C35 siRNA inhibited the growth of SKOV-3 cells after cisplatin treatment ($10\,\mu M$, 3 days). In contrast, no inhibitory effect on cell growth was found in cells transfected with the NTC siRNA. Furthermore, to examine whether knockdown of C35 sensitises the chemo-resistant ovarian cancer cell line, we applied siRNA to knockdown endogenous C35 expression in C13 cells. Cell viability

was evaluated by Trypan blue exclusion assay. The relative cell viability in C35 siRNA-transfected cell after cisplatin treatment was diminished as compared with NTC siRNA-transfected cells (Figure 4F). The result indicated that knockdown of C35 in chemo-resistant cell line can sensitise the response to cisplatin treatment. These data strongly suggest that C35 has a physiological role in the regulation of cell migration and chemo-resistance in ovarian cancer cells.

The interaction between ΔNp73 and C35 reduced the sensitivity of ovarian cancer cells to cisplatin treatment. Because ΔNp73 is recognised as an important mediator of chemo-resistance in various types of cancers (Ishimoto et al, 2002; Zaika et al, 2002; Muller et al, 2005), we next investigated the effect of the C35–ΔNp73 interaction in ovarian cancer cells on the cells' response to cisplatin treatment. The chemo-sensitive ovarian

cancer cell line OV2008 was used as a model. The transient transfection with ΔNp73 significantly reduced the level of apoptosis after cisplatin treatment ($P = 0.0144$). Notably, the co-expression of ΔNp73 and C35 further reduced the number of apoptotic cells (Figure 5A; $P = 0.0006$). Furthermore, the co-expression of C35 and ΔNp73Δ1–76, which showed no binding activity in a co-immunoprecipitation assay, had no significant effect on the level of apoptosis. This result indicates that the interaction between ΔNp73 and C35 is crucial for their ability to contribute to chemo-resistance.

We then examined the effect of ΔNp73 on the cisplatin-induced apoptosis of stable C35-overexpressing clones. A significant reduction in the number of apoptotic cells was observed in ΔNp73-transfected OV-C35-M3 cells compared with OV-MV1 cells and the parental OV2008 cells (Figure 5B; $P < 0.0001$). In addition, we evaluated the effect on cell growth of OV-C35-M3, OV-MV1 and OV2008 cells after cisplatin treatment. We observed that only the OV-C35-M3 cells survived; the OV-MV1 and parental OV2008 cells died following the cisplatin treatment (Figure 5C). These observations further support the roles of C35 and ΔNp73 in promoting the chemo-resistance of ovarian cancer.

C35–ΔNp73 activated AKT and enhanced the expression of NFκB p65. To examine one mechanistic pathway that might be responsible for the inhibition of cisplatin-induced apoptosis, the protein expression of AKT was studied. We observed that cisplatin treatment induced the expression of total AKT in parental OV2008 and OV-MV1 cells (Figure 6A). In contrast, AKT expression was increased in OV-C35-M3 cells before cisplatin treatment, suggesting that the stable expression of C35 enhanced the basal level of AKT expression in OV2008 cells. We next investigated the AKT

activity in these cells by evaluating AKT (S473) phosphorylation. Before cisplatin treatment, higher p-AKT levels were observed in OV-C35-M3 cells than in OV2008 and OV-MV1 cells. Interestingly, the transfection with ΔNp73 further enhanced the AKT phosphorylation in OV-C35-M3 cells (1.2-fold) but not in OV2008 (0.6-fold) or OV-MV1 (0.7-fold) cells. After cisplatin treatment, AKT phosphorylation was dramatically enhanced in ΔNp73-transfected OV-C35-M3 cells (2.8-fold) compared with OV2008 (1.2-fold) and OV-MV1 cells (0.8-fold) (Figure 6A).

Because NFκB is one of the major targets of activated AKT and has been suggested to promote cellular resistance to anticancer drugs, we examined the level of NFκB expression in OV2008, OV-MV1 and OV-C35-M3 cells. Before cisplatin treatment, higher NFκB p65 expression was found in OV-C35-M3 cells than in OV-MV1 or parental OV2008 cells. After cisplatin treatment, we observed that NFκB expression was greatly enhanced in OV-C35-M3 cells. The transfection of OV-C35-M3 cells with ΔNp73 markedly activated the expression of NFκB in response to treatment with cisplatin (Figure 6A).

To determine whether the activation of AKT by C35 is regulated specifically by the PI3K-AKT pathway, the levels of p-AKT and total AKT were evaluated in OV2008, OV-MV1 and OV-C35-M3 cells. Cisplatin treatment alone enhanced the levels of p-AKT in all cell lines tested, and the greatest enhancement was observed in OV-C35-M3 cells. However, the combination of cisplatin and a PI3K inhibitor (LY294002) dramatically reduced the p-AKT levels to very low levels in all cells tested (Figure 6B). Because the increase in AKT activity mediated by C35 in response to cisplatin could be inhibited by LY294002, it can be hypothesised that C35 enhanced the AKT activity in response to cisplatin specifically via the PI3K-AKT signalling pathway.
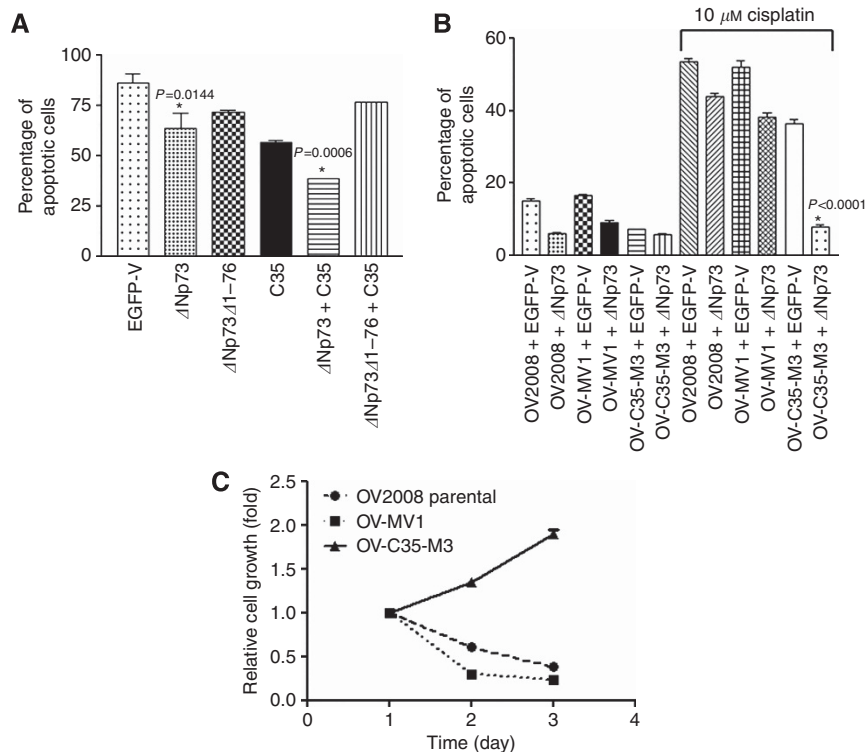

Figure 5. (**A**) OV2008 cells were transiently transfected with the indicated plasmids. Transfected cells were treated with 10 μM cisplatin. After 72 h, the cells were fixed, and the apoptotic cells were subjected to terminal deoxynucleotidyl transferase-mediated dUTP nick end labelling (TUNEL) assays. (**B**) OV-C35-M3, OV-MV1 and parental OV2008 cells were transfected with a control vector or ΔNp73. The transfected cells were treated with either DMSO or 10 μM cisplatin for 72 h. The cells were then fixed, and the apoptotic cells were identified using the TUNEL assay. (**C**) Cell proliferation in OV-C35-M3, OV-MV-1 and parental OV2008 cells was evaluated after cisplatin (10 μM) treatment using an XTT assay.
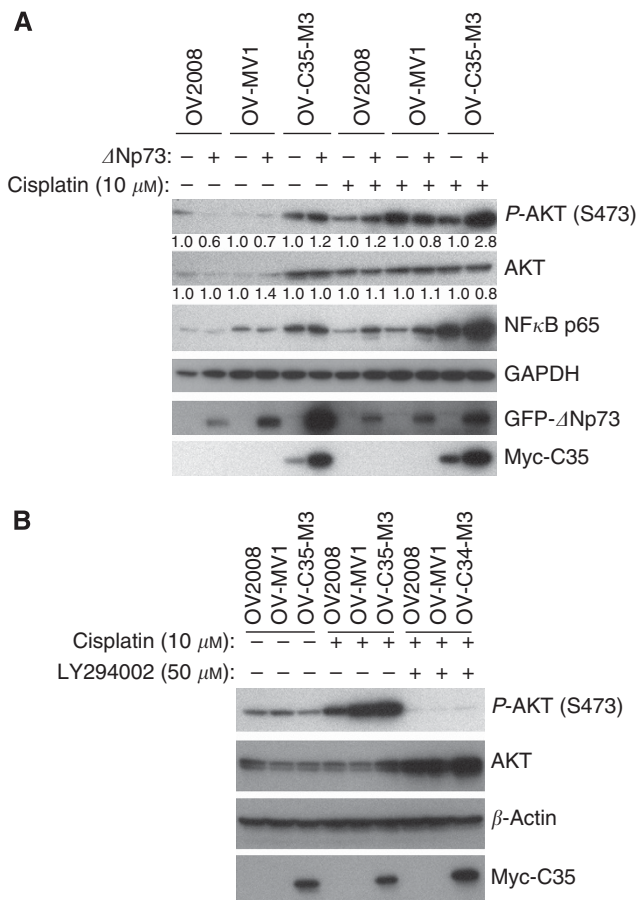
A

B

Figure 6. (**A**) C35 and ΔNp73 synergistically activated AKT and enhanced NFκB p65 expression. OV-C35-M3, OV-MV1 and OV2008 cells were transfected with a control vector or ΔNp73. The expression levels of GFP-ΔNp73 and Myc-C35 were evaluated using anti-GFP and anti-Myc antibodies, respectively. Transfected cells were treated with DMSO or 10 μM cisplatin. AKT activation was evaluated based on the level of phosphorylation at serine 473. The AKT, p-AKT (S473) and NFκB p65 levels were examined by western blotting. GADPH was probed as a loading control. The values below the blots represent the change in protein expressions of the ΔNp73-transfected cells normalised to the expression in the control vector-transfected cells. (**B**) OV-C35-M3, OV-MV1 and OV2008 cells were treated with DMSO, cisplatin alone or a combination of cisplatin and LY294002 for 24 h. The AKT and p-AKT (S473) levels were examined by western blotting. Myc-C35 was detected with an anti-Myc antibody. β-Actin was probed as a loading control.

C35–ΔNp73 activated nuclear NFκB activity. To examine the enhanced NFκB p65 expression in OV-C35-M3 is correlated with the activation of NFκB p65. The nuclear proteins of OV2008, OV-MV1 and OV-C35-M3 were extracted. The nuclear NFκB activity was evaluated by NFκB p65 ELISA. Consistent with the result of western blot, we observed that nuclear NFκB p65 activity was greatly enhanced in OV-C35-M3 cells after cisplatin (10 μM) treatment whereas no obvious changes were found in OV2008 and OV-MV1 cells (Figure 7A).

We then investigated the subcellular localisation of NFκB p65 in OV-MV1 and OV-C35-M3. Enhanced NFκB p65 expression was found in the nuclear fraction of OV-C35-M3 as compared with OV-MV1 prior cisplatin treatment. Notably, the nuclear NFκB p65 expression was further increased in OV-C35-M3 after cisplatin treatment (Figure 7B).
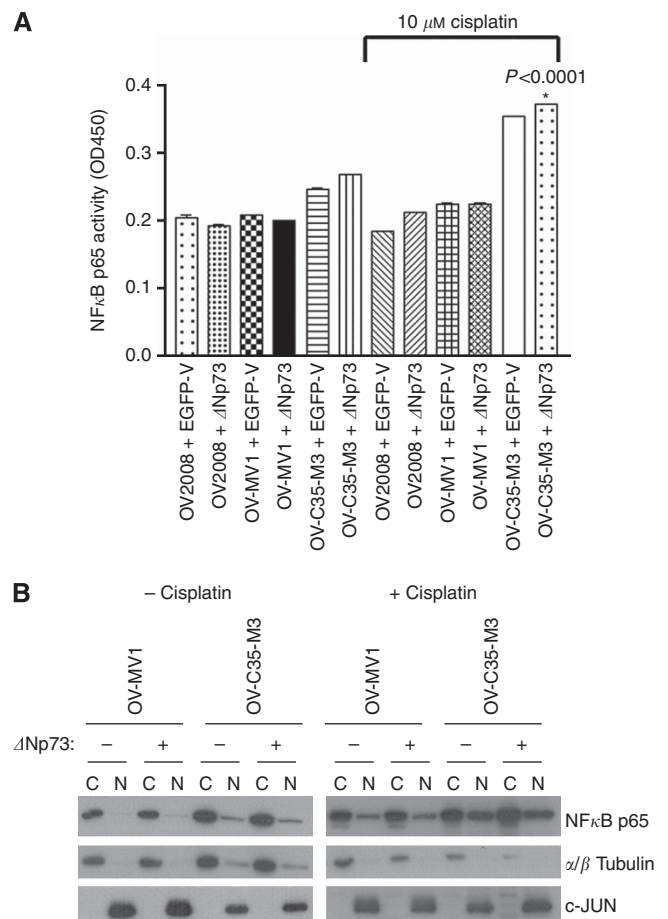
A

B

Figure 7. (**A**) OV-C35-M3, OV-MV1 and OV2008 cells were transfected with a control vector or ΔNp73. Transfected cells were treated with DMSO or 10 μM cisplatin. Nuclear fraction was extracted and the nuclear NFκB activity was examined by NFκB p65 ELISA. (**B**) Subcellular fractionation was performed to separate the cytosolic and nuclear fractions. α/β-Tubulin and c-Jun were used as loading control markers for cytosolic and nuclear fractions, respectively (C: cytosolic fraction; N: nuclear fraction).

DISCUSSION

In the present study, we identified C35 as a novel interacting partner of ΔNp73. We demonstrated for the first time that the interaction between ΔNp73 and C35 enhances the resistance of ovarian cancer cells to cisplatin treatment. A previous study showed that C35 is localised to the cytoplasm (Dasgupta *et al*, 2009). Here, we observed that ectopically expressed C35 also predominantly localised to the cytoplasm in ovarian cancer cells. The co-localisation of C35 and ΔNp73 was observed at the peri-nuclear region of ovarian cancer cells, implying that C35 interacts with ΔNp73 and that this complex exerts its function in the peri-nuclear region.

The amplification of chromosome arm 17q is commonly observed in ovarian cancer cells (Sham *et al*, 2002; Schraml *et al*, 2003). Genes residing in the 17q12 amplicon, including HER/ERBB2 and GRB7, are overexpressed in human cancers, including breast, endometrial and ovarian cancers (Czerwenka *et al*, 1995; Yu and Hung, 2000; Lassus *et al*, 2004; Wang *et al*, 2010). C35 is located near HER/ERBB2 and GRB7 and has also been shown to be overexpressed in breast and prostate cancers (Evans *et al*, 2006; Dasgupta *et al*, 2009; Katz *et al*, 2010). High levels of C35

expression have been found to be associated with *HER2* gene amplification in primary breast cancer tissues (Katz *et al*, 2010). Using quantitative real-time PCR, we showed that the C35 transcript was highly expressed in human ovarian cancer tissues and ovarian cancer cell lines. These data suggest that C35 may function as an oncogene in ovarian cancer. To study the potential positive regulatory role of C35 in ovarian cancer progression, we established stable C35-overexpressing clones. We demonstrated that the upregulation of C35 significantly enhanced cell proliferation and promoted the tumourigenicity of ovarian cancer cells both *in vitro* and *in vivo* (Figure 3). Dasgupta *et al* (2009) reported that C35 promotes the migration and invasion of prostate cancer cells by upregulating MMP-9, UPA and VEGF. Recently, this group further demonstrated that the post-translational modification of the C-terminal prenylation domain of C35 is essential for its membrane association, which facilitates the induction of filopodia formation (Dasgupta *et al*, 2011). However, another study, by Katz *et al* (2010), showed that the MMP-9, UPA and VEGF expression levels are not correlated with C35 expression in breast cancer. These findings suggest that different signalling pathways may be affected by C35 in different types of cancers. Our data confirmed that the overexpression of C35 promoted ovarian cancer cell migration. The downregulation of C35 by siRNA substantially suppressed cell migration and sensitised ovarian cancer cells to cisplatin. Altogether, these results indicate that C35 has an oncogenic role in ovarian cancer.

After C35 was identified and characterised as a novel protein binding partner of ΔNp73 that has a significant role in cancer cell progression and chemo-resistance, we studied the molecular mechanisms underlying the enhancement of ovarian cancer progression by the C35–ΔNp73 interaction. It is well known that the AKT signalling pathway is associated with chemo-resistance in human cancers (Brognard *et al*, 2001; Li *et al*, 2001; Fraser *et al*, 2003; Dan *et al*, 2004; Pommier *et al*, 2004; Kim *et al*, 2005; Abedini *et al*, 2010). TAp73 and ΔNp73 have also been suggested to have important roles in the sensitivity of cancer cells to drug-induced apoptosis (Irwin *et al*, 2003; Vayssade *et al*, 2005; Al-Bahlani *et al*, 2011). Previous studies have demonstrated that ΔNp73 enhances chemo-resistance in various types of cancers (Ishimoto *et al*, 2002; Zaika *et al*, 2002; Muller *et al*, 2005). The downregulation of C35 by siRNA has been proposed to suppress the activation of AKT, whereas the stable overexpression of C35 enhances AKT phosphorylation and NFκB activity in prostate cancer cells (Dasgupta *et al*, 2009). In this study, we observed that ΔNp73 enhanced the chemo-resistance of ovarian cancer cells to cisplatin treatment. Furthermore, the role of C35 in enhancing ΔNp73-mediated chemo-resistance in ovarian cancer was verified by the transient transfection of C35 and ΔNp73 into cisplatin-sensitive OV2008 cells. A significant reduction in apoptosis was observed after cisplatin treatment in ΔNp73 and C35 co-expressing cells. Western blot analysis also revealed that the expression levels of p-AKT and nuclear NFκB p65 were greatly enhanced in ΔNp73 and C35 co-expressing cells treated with cisplatin. Our current findings suggest that the C35–ΔNp73 interaction enhances the activation of AKT and the activity of NFκB after cisplatin treatment, ultimately diminishing the apoptotic response to cisplatin.

In summary, the findings presented herein delineate a possible mechanistic pathway for the promotion of oncogenesis in ovarian cancer by the C35–ΔNp73 complex. C35 is highly expressed in ovarian cancer cells and tumour tissues. C35 potentiates the functions of ΔNp73 in tumour progression and chemo-resistance by activating AKT and nuclear NFκB p65. This study is the first to illustrate a possible mechanism by which ΔNp73 and C35 contribute to the chemo-resistance of ovarian cancer cells. Further studies of the functional importance of the C35–ΔNp73 interaction will be essential to gain better insight into the roles of these proteins in ovarian cancer.

REFERENCES

Abedini MR, Muller EJ, Bergeron R, Gray DA, Tsang BK (2010) Akt promotes chemoresistance in human ovarian cancer cells by modulating cisplatin-induced, p53-dependent ubiquitination of FLICE-like inhibitory protein. *Oncogene* **29**(1): 11–25.

Al-Bahlani S, Fraser M, Wong AY, Sayan BS, Bergeron R, Melino G, Tsang BK (2011) P73 regulates cisplatin-induced apoptosis in ovarian cancer cells via a calcium/calpain-dependent mechanism. *Oncogene* **30**(41): 4219–4230.

Asselin E, Mills GB, Tsang BK (2001) XIAP regulates Akt activity and caspase-3-dependent cleavage during cisplatin-induced apoptosis in human ovarian epithelial cancer cells. *Cancer Res* **61**(5): 1862–1868.

Brognard J, Clark AS, Ni Y, Dennis PA (2001) Akt/protein kinase B is constitutively active in non-small cell lung cancer cells and promotes cellular survival and resistance to chemotherapy and radiation. *Cancer Res* **61**(10): 3986–3997.

Czerwenka K, Lu Y, Heuss F (1995) Amplification and expression of the c-erbB-2 oncogene in normal, hyperplastic, and malignant endometria. *Int J Gynecol Pathol* **14**(2): 98–106.

Dan HC, Jiang K, Coppola D, Hamilton A, Nicosia SV, Sebti SM, Cheng JQ (2004) Phosphatidylinositol-3-OH kinase/AKT and survivin pathways as critical targets for geranylgeranyltransferase I inhibitor-induced apoptosis. *Oncogene* **23**(3): 706–715.

Dasgupta S, Cushman I, Kpetemey M, Casey PJ, Vishwanatha JK (2011) Prenylated C17ORF37 induces filopodia formation to promote cell migration and metastasis. *J Biol Chem* **286**(29): 25935–25946.

Dasgupta S, Wasson LM, Rauniyar N, Prokai L, Borejdo J, Vishwanatha JK (2009) Novel gene C17orf37 in 17q12 amplicon promotes migration and invasion of prostate cancer cells. *Oncogene* **28**(32): 2860–2872.

Evans EE, Henn AD, Jonason A, Paris MJ, Schiffhauer LM, Borrello MA, Smith ES, Sahasrabudhe DM, Zauderer M (2006) C35 (C17orf37) is a novel tumor biomarker abundantly expressed in breast cancer. *Mol Cancer Ther* **5**(11): 2919–2930.

Fraser M, Leung BM, Yan X, Dan HC, Cheng JQ, Tsang BK (2003) p53 is a determinant of X-linked inhibitor of apoptosis protein/Akt-mediated chemoresistance in human ovarian cancer cells. *Cancer Res* **63**(21): 7081–7088.

Irwin MS, Kondo K, Marin MC, Cheng LS, Hahn WC, Kaelin Jr WG (2003) Chemosensitivity linked to p73 function. *Cancer Cell* **3**(4): 403–410.

Ishimoto O, Kawahara C, Enjo K, Obinata M, Nukiwa T, Ikawa S (2002) Possible oncogenic potential of DeltaNp73: a newly identified isoform of human p73. *Cancer Res* **62**(3): 636–641.

Kaghad M, Bonnet H, Yang A, Creancier L, Biscan JC, Valent A, Minty A, Chalon P, Lelias JM, Dumont X, Ferrara P, McKeon F, Caput D (1997) Monoallelically expressed gene related to p53 at 1p36, a region frequently deleted in neuroblastoma and other human cancers. *Cell* **90**(4): 809–819.

Katz E, Dubois-Marshall S, Sims AH, Faratian D, Li J, Smith ES, Quinn JA, Edward M, Meehan RR, Evans EE, Langdon SP, Harrison DJ (2010) A gene on the HER2 amplicon, C35, is an oncogene in breast cancer whose actions are prevented by inhibition of Syk. *Br J Cancer* **103**(3): 401–410.

Kim D, Dan HC, Park S, Yang L, Liu Q, Kaneko S, Ning J, He L, Yang H, Sun M, Nicosia SV, Cheng JQ (2005) AKT/PKB signaling mechanisms in cancer and chemoresistance. *Front Biosci* **10**: 975–987.

Lassus H, Leminen A, Vayrynen A, Cheng G, Gustafsson JA, Isola J, Butzow R (2004) ERBB2 amplification is superior to protein expression status in predicting patient outcome in serous ovarian carcinoma. *Gynecol Oncol* **92**(1): 31–39.

Leung TH, Ching YP, Yam JW, Wong CM, Yau TO, Jin DY, Ng IO (2005) Deleted in liver cancer 2 (DLC2) suppresses cell transformation by means of inhibition of RhoA activity. *Proc Natl Acad Sci USA* **102**(42): 15207–15212.

Leung TH, Ngan HY (2010) Interaction of TAp73 and breast cancer-associated gene 3 enhances the sensitivity of cervical cancer cells in response to irradiation-induced apoptosis. *Cancer Res* **70**(16): 6486–6496.

Li J, Feng Q, Kim JM, Schneiderman D, Liston P, Li M, Vanderhyden B, Faught W, Fung MF, Senterman M, Korneluk RG, Tsang BK (2001) Human ovarian cancer and cisplatin resistance: possible role of inhibitor of apoptosis proteins. *Endocrinology* **142**(1): 370–380.

Liu SS, Chan KY, Cheung AN, Liao XY, Leung TW, Ngan HY (2006) Expression of deltaNp73 and TAp73alpha independently associated with radiosensitivities and prognoses in cervical squamous cell carcinoma. *Clin Cancer Res* **12**(13): 3922–3927.

Muller M, Schilling T, Sayan AE, Kairat A, Lorenz K, Schulze-Bergkamen H, Oren M, Koch A, Tannapfel A, Stremmel W, Melino G, Krammer PH (2005) TAp73/Delta Np73 influences apoptotic response, chemosensitivity and prognosis in hepatocellular carcinoma. *Cell Death Differ* **12**(12): 1564–1577.

Muscolini M, Cianfrocca R, Sajeva A, Mozzetti S, Ferrandina G, Costanzo A, Tuosto L (2008) Trichostatin A up-regulates p73 and induces Bax-dependent apoptosis in cisplatin-resistant ovarian cancer cells. *Mol Cancer Ther* **7**(6): 1410–1419.

Pommier Y, Sordet O, Antony S, Hayward RL, Kohn KW (2004) Apoptosis defects and chemotherapy resistance: molecular interaction maps and networks. *Oncogene* **23**(16): 2934–2949.

Righetti SC, Perego P, Carenini N, Zunino F (2008) Cooperation between p53 and p73 in cisplatin-induced apoptosis in ovarian carcinoma cells. *Cancer Lett* **263**(1): 140–144.

Sasaki H, Sheng Y, Kotsuji F, Tsang BK (2000) Down-regulation of X-linked inhibitor of apoptosis protein induces apoptosis in chemoresistant human ovarian cancer cells. *Cancer Res* **60**(20): 5659–5666.

Schraml P, Schwerdtfeger G, Burkhalter F, Raggi A, Schmidt D, Ruffalo T, King W, Wilber K, Mihatsch MJ, Moch H (2003) Combined array comparative genomic hybridization and tissue microarray analysis suggest PAK1 at 11q13.5-q14 as a critical oncogene target in ovarian carcinoma. *Am J Pathol* **163**(3): 985–992.

Sham JS, Tang TC, Fang Y, Sun L, Qin LX, Wu QL, Xie D, Guan XY (2002) Recurrent chromosome alterations in primary ovarian carcinoma in Chinese women. *Cancer Genet Cytogenet* **133**(1): 39–44.

Tsao SW, Wong N, Wang X, Liu Y, Wan TS, Fung LF, Lancaster WD, Gregoire L, Wong YC (2001) Nonrandom chromosomal imbalances in human ovarian surface epithelial cells immortalized by HPV16-E6E7 viral oncogenes. *Cancer Genet Cytogenet* **130**(2): 141–149.

Vayssade M, Haddada H, Faridoni-Laurens L, Tourpin S, Valent A, Benard J, Ahomadegbe JC (2005) P73 functionally replaces p53 in Adriamycin-treated, p53-deficient breast cancer cells. *Int J Cancer* **116**(6): 860–869.

Wang Y, Chan DW, Liu VW, Chiu P, Ngan HY (2010) Differential functions of growth factor receptor-bound protein 7 (GRB7) and its variant GRB7v in ovarian carcinogenesis. *Clin Cancer Res* **16**(9): 2529–2539.

Yu D, Hung MC (2000) Overexpression of ErbB2 in cancer and ErbB2-targeting strategies. *Oncogene* **19**(53): 6115–6121.

Zaika AI, Slade N, Erster SH, Sansome C, Joseph TW, Pearl M, Chalas E, Moll UM (2002) DeltaNp73, a dominant-negative inhibitor of wild-type p53 and TAp73, is up-regulated in human tumors. *J Exp Med* **196**(6): 765–780.